

*promoting access to White Rose research papers*



**Universities of Leeds, Sheffield and York**  
**<http://eprints.whiterose.ac.uk/>**

---

This is an author produced version of a paper published in **Surface and Coatings Technology**.

White Rose Research Online URL for this paper:  
<http://eprints.whiterose.ac.uk/4956/>

---

**Published paper**

Liskiewicz, T., Fouvry, S. and Wendler, B. (2003) *Impact of variable loading conditions on fretting wear*. Surface and Coatings Technology, 163-164 . pp. 465-471. [http://dx.doi.org/10.1016/S0257-8972\(02\)00643-6](http://dx.doi.org/10.1016/S0257-8972(02)00643-6)

---

# Impact of variable loading conditions on fretting wear

T. LISKIEWICZ<sup>a,b</sup>, S. FOUVRY<sup>a\*</sup>, B. WENDLER<sup>b</sup>

<sup>a</sup> LTDS, UMR CNRS 5513, Ecole Centrale de Lyon, 36 Avenue Guy de Collongue

BP163, 69131 Ecully, France

<sup>b</sup> Institute of Materials Science and Technology, Technical University of Lodz,

ul. Stefanowskiego 1, 90 924 Lodz, Poland

\* *Corresponding author: siegfried.fouvry@ec-lyon.fr*

**Abstract :** Fretting is considered as a specific type of reciprocating sliding. It is defined as a small displacement amplitude oscillatory motion between two solids in contact, usually induced by vibrations. Depending on the loading conditions (displacement amplitudes, normal loading), fretting causes damage by surface fatigue and wear induced by debris formation. To prevent such damage, numerous hard coatings have been developed which improve the wear resistance of contacts. However, one difficulty is to estimate how long it will be before the coating wears through. Studies have been conducted to analyze the effect of displacement amplitude, normal force or ambient atmosphere, but usually under constant loading conditions. Such a situation is far from real operating components, where elements are subjected to variable loadings implying variable displacement amplitudes. To predict the durability of a coating under variable fretting displacements, wear depth is quantified as a function of the maximum accumulated dissipated energy density by derivation from a global energy wear approach. This model is compared to TiC vs. alumina fretting experiments. Very good correlation is observed between the prediction and the wear depth, independently of the applied variable amplitude sequences. An equivalent “Miner-Energy” wear model is introduced which permits the durability of the coating to be estimated.

## **Keywords**

Fretting wear, reciprocating sliding, TiC coating, variable amplitudes, dissipated energy, energy wear approach.

## **1. Introduction**

Wear induced by fretting [1] is a process that occurs in a nominally immovable junction of two elements as, for example, in a key or an interference or a riveted or a screw joint. It is due to micro-displacements of mated machine elements. The displacement between adjacent surfaces is generally caused by a machine motion or oscillations or vibrations. To study such phenomena, fretting tests are carried out in a variety of displacement amplitude ranges [2,3,4,5,6], but usually under constant loading conditions. Such a situation is very different from real operating conditions of mechanical devices, where elements are working with various speeds or frequencies or at different thermal stresses and under a variety of loading conditions. All these parameters directly influence the fretting displacement amplitude.

In this work we present the results of tests performed on hard titanium carbide coating under constant and variable loading conditions. The resistance of such a coating to fretting wear has been established in the literature [4,5]. The aim of the present paper is to determine how the TiC coating behaves under variable displacement amplitudes and if it is possible to predict the lifetime of a coating.

To quantify the wear process, a global energy approach was linked to the total wear volume, whereas to predict the lifetime of a coating a dissipated energy density approach was developed.

## **2. Experiments**

### *2.1 Fretting Apparatus*

Fretting tests were carried out using an electrodynamic shaker activating a specific fretting rig illustrated in Figure 1.

Tests were conducted in a closed chamber where both the ambient and relative humidity are controlled. The normal force ( $P$ ) is kept constant, while the tangential force ( $Q$ ) and displacement ( $\delta$ ) are recorded. A reciprocating movement with a constant speed was imposed. Thus the fretting loop  $Q - \delta$  can be drawn to extract quantitative variables inducing the dissipated energy ( $E_d$ ) (i.e. . the area of the hysteresis)[6], the sliding amplitude ( $\delta_g$ ), the displacement amplitude ( $\delta_*$ ), and the tangential force amplitude ( $Q_*$ ). To obtain a dynamic overview of the fretting test, the fretting cycles are superimposed, resulting in the fretting log. The cumulated dissipated energy is defined by the sum :

$$\Sigma E_d = \sum_{i=1}^N E_{di} \quad (1)$$

A mean friction value defined over the whole fretting cycle appears more pertinent to quantify the wear. An energy friction coefficient is introduced.

$$\mu_e = \frac{E_d}{4 \cdot P \cdot \delta_g} \quad (2)$$

Thus, the average value over the test duration is defined from :

$$\bar{\mu}_e = \frac{1}{N} \sum_{i=1}^N \frac{E_{di}}{4 \cdot \delta_{gi} \cdot P_i} \quad (3)$$

## 2.2 Material

A high speed steel VANADIS 23 (1,28 wt.% C; 4,2 wt.% Cr; 5,0 wt.% Mo; 6,4 wt.% W and 3,1 wt.% V) was used as a substrate for the TiC coating. A series of 10x10x10mm specimens were cut from the steel. Average surface roughness parameter  $R_a$  for the substrate and coating was 0,2 $\mu$ m. TiC coating was deposited onto one of the end faces of the samples by a two step indirect method [7]. First, a metallic Ti layer was deposited by magnetron sputtering and secondly the samples were annealed for one hour at 1423K in a vacuum furnace with a residual pressure of 10<sup>-4</sup>Pa. Then, the specimens were oil quenched and tempered twice at 833K (1 hour each time). During the annealing step the carbon atoms from the 6-5-2 steel substrate diffused to the titanium coating turning it into a titanium carbide one. A

polycrystalline alumina ball with a 12,7mm radius and an  $R_a$  lower than  $0,01\mu\text{m}$  was used as a counter body. Mechanical and surface properties of materials are summarized in Table 1.

### *2.3 Test Conditions*

Fretting tests were carried out under a 100 N normal loading leading to maximum Hertzian pressure around 1400 MPa. A reciprocating motion with a constant speed, a 5Hz frequency and a number of fretting cycles from 5000 to 25000 was applied. Tests were conducted under constant relative humidity fixed at 50% and  $20^\circ\text{C}$ . The gross slip conditions were maintained throughout the test [8]. During the tests five different loading conditions were applied: two with a constant 50 or  $100\mu\text{m}$  displacement amplitude and three with variable amplitudes. A “bloc” of variable amplitudes is defined by a given number of cycles with  $50\mu\text{m}$  displacement amplitude followed by a similar number of cycles with  $100\mu\text{m}$  amplitude. The test duration, characterized by a total number of cycles  $N$ , may be divided in one, two and four blocs defining the studied  $(50/100)\mu\text{m}_{x1}$ ,  $(50/100)\mu\text{m}_{x2}$  and  $(50/100)\mu\text{m}_{x4}$  sequences respectively.

The wear volume of the fretting scars was measured using 2D profilometry equipment. For each wear scar profiles along and across the sliding direction were obtained. To determine the total wear volume, a simplified integration was used [9]. Prior to testing, specimens were cleaned with acetone.

### *3. Tribological Behaviour*

Figure 3a shows the evolution of the average friction coefficient as a function of the total number of cycles imposed. It stabilizes around 0.5 and remains constant independently of the displacement amplitudes or the displacement sequences. Thus for the studied loading condition, the sliding amplitude (constant or variable) has no influence on the friction behavior. This stability is indirectly related to the low impact of the third body for such tribosystem. Figure 3b confirms that the debris which present a powder structure are easily ejected from the interface contrary to metal or polymer contacts [10].

#### 4. Global wear analysis

Investigations of various (constant or variable) loading conditions confirm a correlation between the wear volume extension of TiC coating and the applied displacement amplitudes (Fig. 4).

For any particular numbers of cycles, the 100  $\mu\text{m}$  amplitude condition causes the greatest wear while that of 50 $\mu\text{m}$  causes the least. All three variable loading conditions result in intermediate wear volumes.

To quantify fretting wear resistance we used an energy approach [6, 11], in which the wear volume of degraded material is related to the shear work (i.e. accumulated energy) dissipated in the contact area.

The volume of removed material  $W_V$  then becomes a function of accumulated dissipated energy  $\Sigma E_d$  and wear resistance is expressed by the energy wear coefficient:

$$\alpha_V = \frac{W_V}{\Sigma E_d} [\mu\text{m}^3 / \text{J}] \quad (4)$$

Fig. 5 shows that when the energy approach is applied, one global energy wear coefficient common to all the loading conditions can be derived. For the tested TiC coating we calculate the energy wear coefficient  $\alpha_V = 415 \mu\text{m}^3/\text{J}$ , which corresponds to a good wear resistance among the thin coatings [5].

#### 5. Local wear analysis

The results presented in the previous section demonstrate that the global energy concept allows the wear volume of the TiC coating under various loading conditions to be described with a single value of energy coefficient. The value of this coefficient characterizes the wear resistance of the coating. Nevertheless, in thin film applications, the main difficulty in extending the lifetime of the components is not loss of volume but wear depth evolution. This is the parameter that determines the longevity of a particular coating.

### 5.1 Constant loading conditions

Transposing previous local energy developments [9], a dissipated energy density approach is derived. In a first approximation the Hertzian shear work distribution could be utilized but due to rapid wear of the interface and its constant extension a mean pressure description appears to be more representative [12].

The dissipated energy density at the center of the contact during the “ $i^{th}$ ” cycle is expressed by

$$E_{dh(i)} (\text{J} / \text{m}^2) = 4 \cdot \delta_{0(i)} \cdot \mu_{e(i)} \cdot P_{m(i)} \quad (5)$$

with the mean pressure  $p_{m(i)}$  equal to

$$P_{m(i)} = \frac{P}{\pi \cdot r_{s(i)}^2} \quad (6)$$

where  $r_{s(i)}$  is a real wear scar radius for the “ $-i^{th}$ ” fretting cycle, determined by optical measurements and projected by the evolution of  $r_s$  as a function of the accumulated global dissipated energy given on Fig. 6. The dissipated energy dependence of the wear scar radius extension is in fact a direct consequence of the wear volume increase with the accumulated dissipated energy.

For each test the local energy density is added up, which leads to the cumulative maximum dissipated energy density at the center of the contact.

$$\Sigma E_{dh} = \sum_{i=1}^N E_{dh(i)} \quad (7)$$

Based on that approach we could establish the accumulated dissipated energy density. Fig.7 presents the values of the wear depth for each test, plotted against the corresponding maximum accumulated dissipated energy density. A linear evolution is observed which confirms the reliability of the energy approach.

### 5.2 Variable displacement amplitude

As shown in Fig.8, the evolution of the dissipated energy density during a fretting test is related to changes in displacement amplitude and the evolution of contact radius ( $r_s$ ) during the test.

For each test performed under variable loading conditions, cumulative dissipated energy density was calculated in the same manner as described above. Subsequently, the values of the wear scar depth measured in each test were plotted against the corresponding maximum accumulated dissipated energy density calculated for that test (Fig.9).

It still confirms the reliability of the dissipated energy density approach to predict wear depth of tested coating. Linear regression leads to a  $\beta_V$  value equals to  $\beta_V = 1200.6 \mu\text{m}^3 / \text{J}$  for the studied TiC/alumina contact.

Therefore the wear depth extension (h) can be expressed through the relation:

$$h = \beta_V \cdot \Sigma E_{dh} \quad (8)$$

### 5.3 Predicting when the substrate will be reached

The study confirms the energy approach as a convenient approach to predict the lifetime of a coating. Hence for a given coating thickness 't' we can identify the critical dissipated energy density 'E<sub>dhc</sub>' related to the moment when the substrate is reached:

$$E_{dhc} = \frac{t}{\beta_V} \quad (9)$$

The TiC studied coating thickness is 1,8 $\mu\text{m}$  witch leads to  $E_{dhc} = 0.00151 \text{ J}/\mu\text{m}^2$ .

To validate the stability of such a predictive approach, test were continued until the substrate was reached. The coating fracture was indicated by a discontinuity of the friction coefficient. For the particular test presented in Fig. 10, this discontinuity appeared after 21000 cycles, which corresponds to a critical value  $E_{dhc} = 0.00161 \text{ J}/\mu\text{m}^2$ . It is very close to the predicted



value. The small difference can be imputed to the establishment of the alumina/steel contact marking the friction discontinuity.

#### 5.4 Equivalent “Energy - Wohler” Wear approach

To establish when the substrate is reached under variable loading conditions we have to consider the accumulated energy dissipated density under different applied amplitudes. When the displacement amplitude increases, the value of  $E_{dhc}$  is higher and the coating is damaged quicker. The energy concept is relevant because of its additive property. Regarding the previous analysis the wear through the coating can be formalized by :

$$\sum_{i=1}^N E_{dh}(i) \geq E_{dhc} \quad (10)$$

If the normal force and friction coefficient remain constant, as observed for the current study, the general expression can be simplified as a function of the displacement amplitude and the applied number of cycles. This energy approach permits to model a “displacement – fretting cycles chart ” previously introduced by C. Langlade et al [13]. Although, the present energy concept, by integrating most of the loading variables, appears more “universal” and allows to extrapolate an equivalent “Energy - Wohler” fretting wear chart (Fig.11).

Assuming constant pressure and shear fields, an equivalent “Miner” wear-coating approach can be derived. The substrate reaching condition is then expressed by the relation :

$$\sum \frac{n_i}{N_i} = 1 \quad (11)$$

Where,  $n_i$  is the number of cycles applied at the -i- th condition of displacement amplitude and  $N_i$  the number of cycles associated to the substrate reaching for the corresponding displacement amplitude.

## 6. Conclusion

The tribological behavior of a TiC coating has been evaluated under constant and variable loading conditions. The following conclusions can be drawn:

- The global wear energy approach permit the wear volume removal as a function of the accumulated dissipated energy to be predicted independently of the displacement amplitude (constant or variable).
- To predict the wear depth extension that appears to be the controlling factor of the coating duration, an energy density approach is derived. It consists in relating the wear depth extension as a function of the maximum accumulated dissipated energy density.
- This local energy approach implies that the mean pressure evolution related to the contact area extension must be considered instead of the Hertzian formalism. The contact radius extension was formalized through the dissipated energy in the contact.
- By introducing the wear energy density coefficient  $\beta_v$ , a critical value of dissipated energy density '  $E_{dhc}$  ' can be determined, which leads directly to the coating lifetime under constant or variable displacement amplitudes.
- From this formalism and considering the constant normal force and friction, an equivalent „Energy-Wohler” wear chart is introduced. It expresses the moment when the substrate is reached as a function of the displacement amplitude and the number of fretting cycles. This approach is extended to the variable amplitude conditions introducing a corresponding „Energy-Miner” wear depth approach, thus allowing the accumulated wear damages to be formalised.

Displaying a very strong stability to quantify the wear damage of hard coating this dissipated energy density approach must be compared to variable ambient conditions and also more complex systems like metal-metal contacts which are significantly controlled by adhesion phenomena.

### **Ackowlegments**

The authors would like to thank the MIRA program of the Region Rhone Alpes for the financial support of this work.

## References

- [1] R.B. Waterhouse (ed.), Fretting Fatigue, Applied Science, London, 1981.
- [2] P.L. Ko, M.-C. Taponat, R. Pfaifer, Tribology International, 34 (2001) 7.
- [3] Q.Y. Liu, Z.R. Zhou, Wear, 239 (2000) 237.
- [4] S. Fouvry, Ph. Kapsa, L. Vincent, B. Wendler, P. Kula, Inzynieria Materialowa, 105 (1998) 990.
- [5] S. Fouvry, Ph. Kapsa, Surface and Coatings Technology, 138 (2001) 141.
- [6] S. Fouvry, Ph. Kapsa, L. Vincent, Wear, 200 (1996) 186.
- [7] B.G. Wendler, Surface and Coating Technology, 100-101 (1998) 276.
- [8] R.D. Mindlin, H. Deresiewicz, J. Appl. Mech., 20 (1953) 327.
- [9] S. Fouvry, Ph. Kapsa, H; Zahouani, L. Vincent, Wear, 203-204 (1997) 393.
- [10] A. Chateauminos, M. Kharrat, A. Krichen, ASTM STP 1367 (2000) 352.
- [11] H. Mohrbaker, B. Blanpain, J.P. Celis and J.R. Roos, Wear 180 (1995) 43.
- [12] E. Sauger, S; Fouvry, L. Ponsonnet, Ph. Kapsa, J. M. Martin, L. Vincent, Wear 245 (2000) 39.
- [13] C. Langlade, B. Vannes, M. Taillandier, M. Pierantoni, Tribology International 34 (2001) 49.

Table 1. Mechanical properties of materials used in studies.

	$E$ (GPa)	$\nu$	Hardness	Thickness ( $\mu\text{m}$ )	$R_a$ ( $\mu\text{m}$ )	$R_e$ (MPa)
<i>VANADIS 23</i>	230	0,3	64 HRC	-	0,2	3400
<i>TiC coating</i>	450	0,2	1100 HV <sub>0,05</sub>	1,8	0,2	-
<i>Alumina ball</i>	370	0,27	2300 HV <sub>0,1</sub>	-	0,01	-

## FIGURE CAPTIONS

Fig. 1 : (a) schematic of the fretting rig, (b) analysis of the fretting cycle, (c) Fretting log.

Fig. 2 : Variable loading conditions : (a) -  $(50/100)\mu\text{m}_{x1}$  ; (b) -  $(50/100)\mu\text{m}_{x2}$  ; (c) -  $(50/100)\mu\text{m}_{x4}$  .

Fig. 3 : (a) Evolution of the mean friction coefficient as a function of the loading conditions; (b) SEM observation of the fretting scar TiC/alumina ( $P=100\text{ N}$ ,  $\delta=\pm 100\mu\text{m}$ , 5000 cycles), most of the debris are ejected from the interface.

Fig. 4 :Wear volume ( $W_v$ ) versus total number of cycles for various loading conditions.

Fig. 5 : Global wear analysis: identification of the energy wear coefficient  $\alpha_v$ .

Fig. 6 : Wear scar radius ( $r_s$ ) versus accumulated dissipated energy ( $\Sigma E_d$ ) - for various loading conditions.

Fig. 7 : Linear correlation between the wear depth ( $h$ ) and the cumulative dissipated energy density ( $\Sigma E_{dh}$ ) for various constant loading conditions.

Fig. 8 : Evolution of the dissipated energy density ( $E_{dh}$ ) during the tests.

Fig. 9 : Local wear analysis: identification of the energy density wear coefficient  $\beta_v$ . A linear evolution is observed independently of the sliding conditions (constant or variable).

Fig. 10 : Evolution of maximum dissipated energy density ( $E_{dh}$ ) and friction coefficient ( $\mu$ ) during the test as a function of the number of cycles.

Fig. 11 : Energy Wohler wear chart (TiC/alumina) (illustration of the accumulated energy wear damage approach).

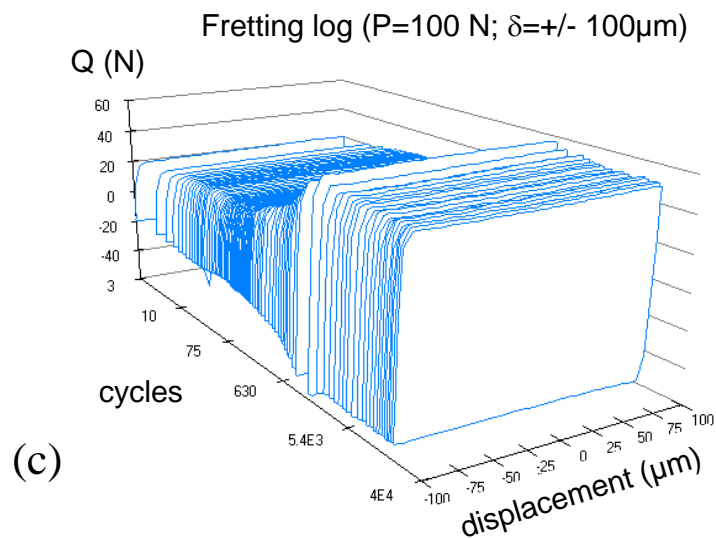
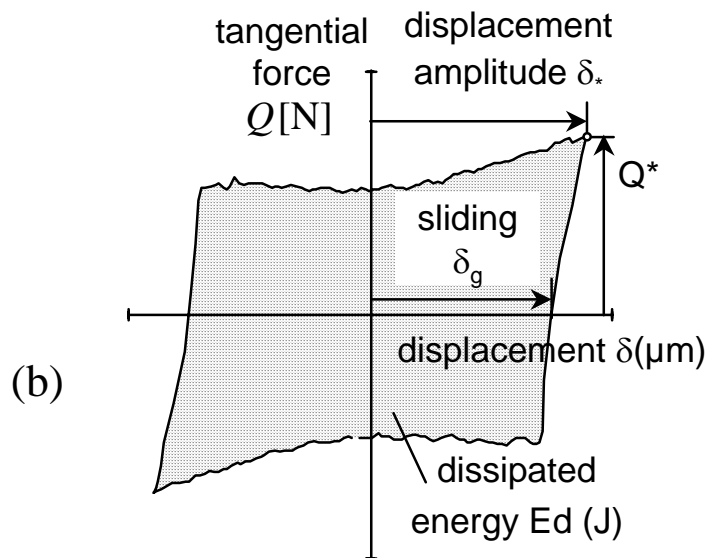
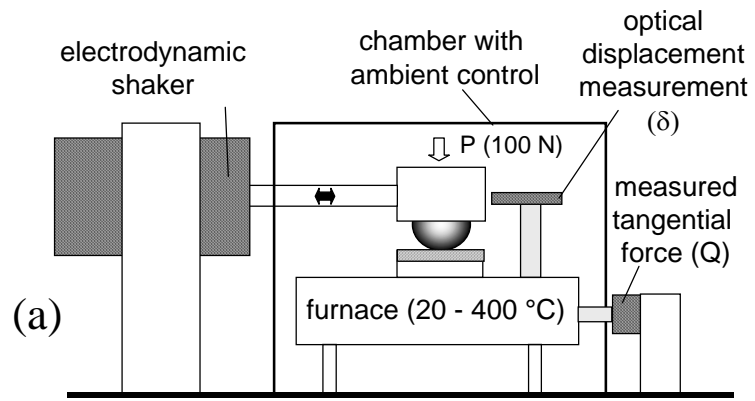


Fig. 1

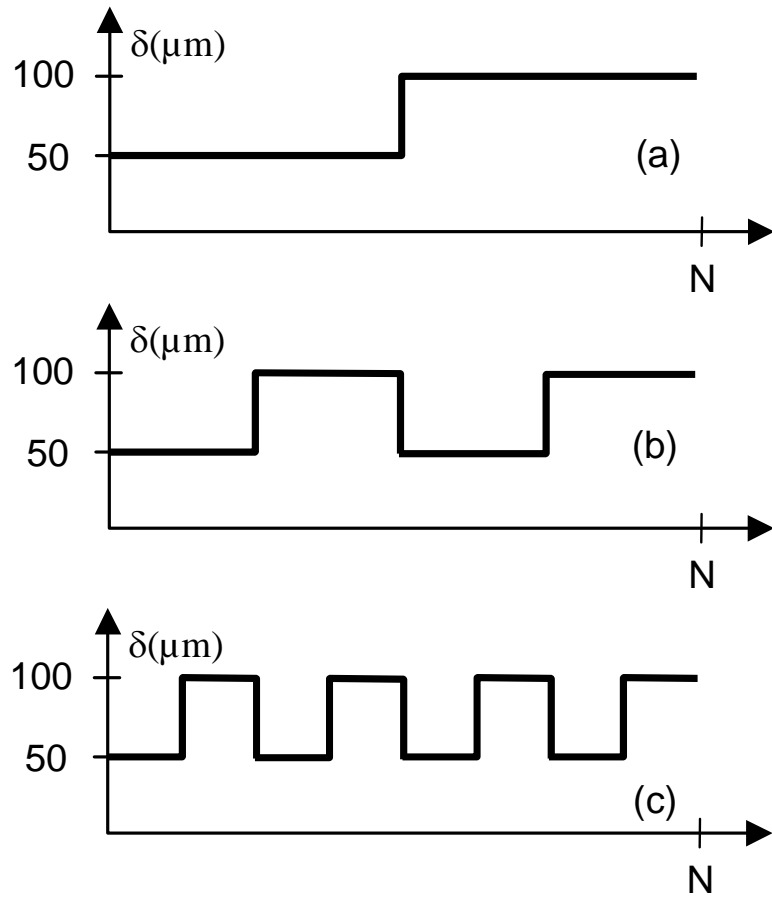
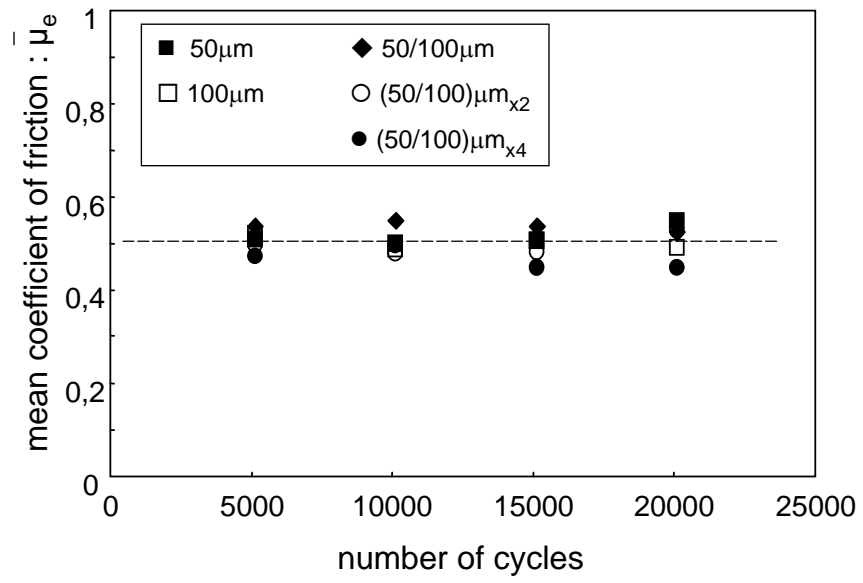
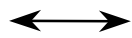
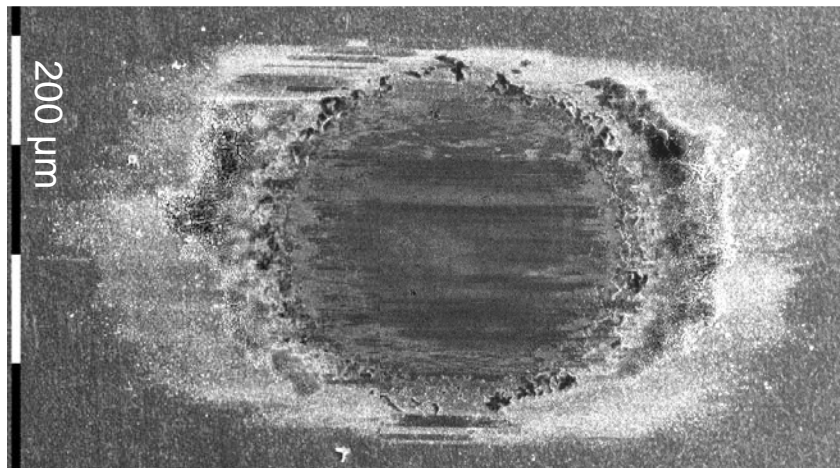


Fig. 2



(a)



(b)

Fig. 3



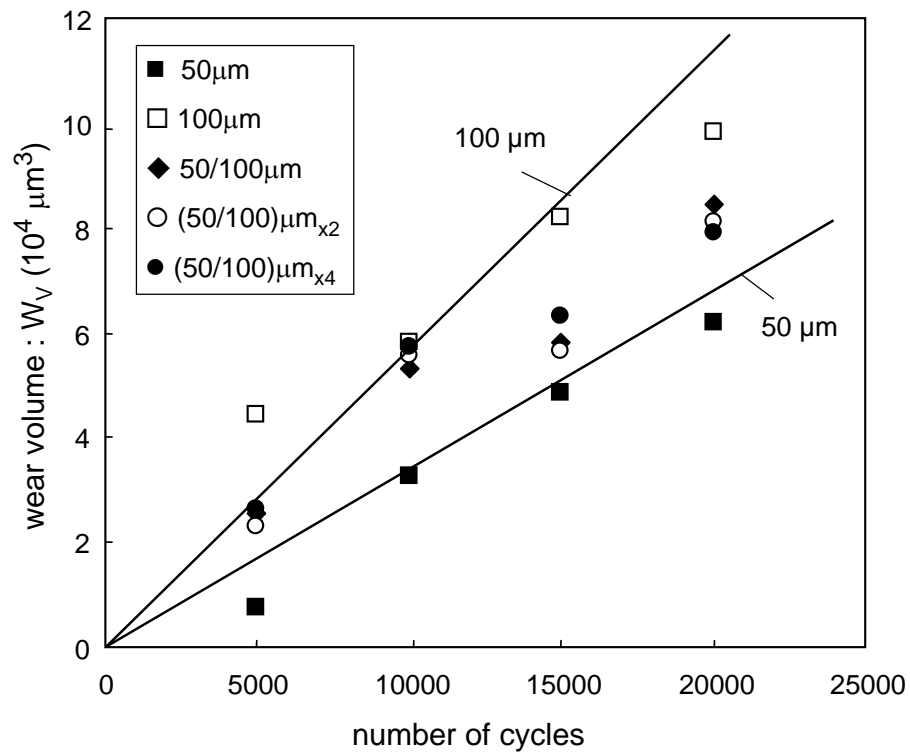


Fig. 4

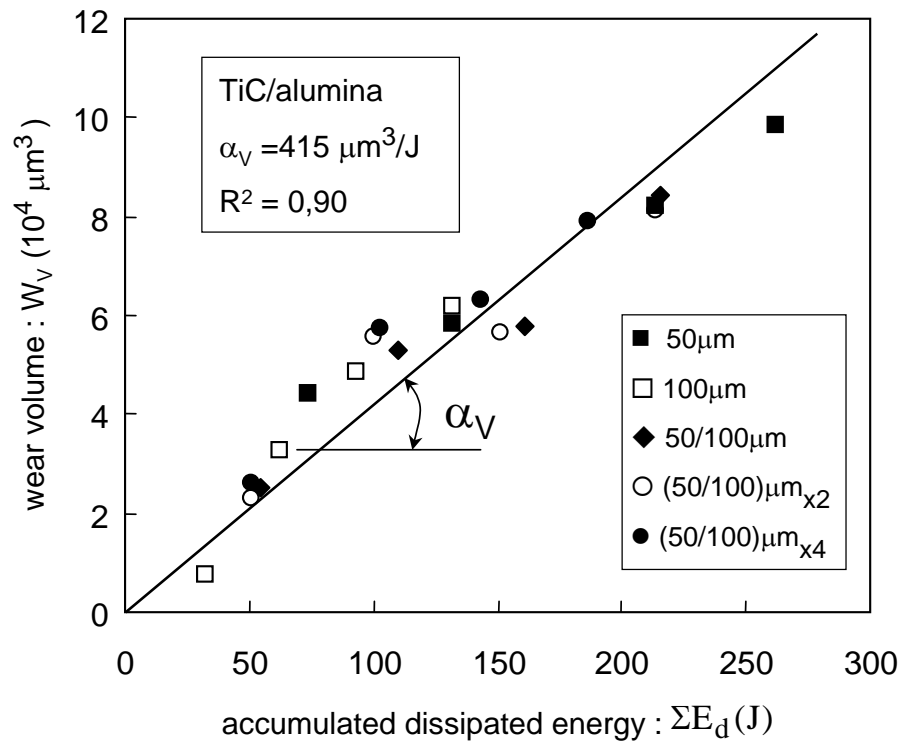


Fig. 5

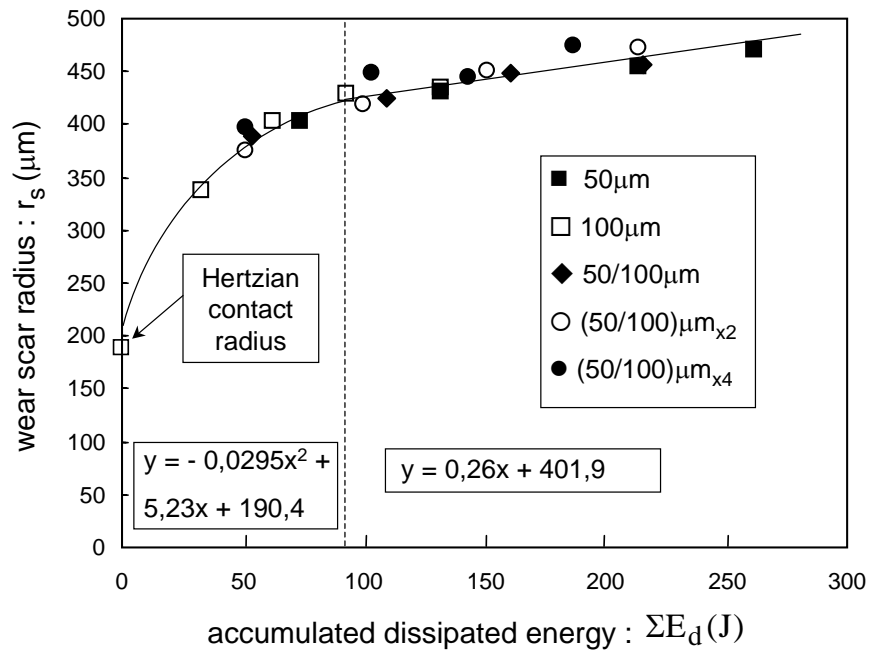


Fig. 6

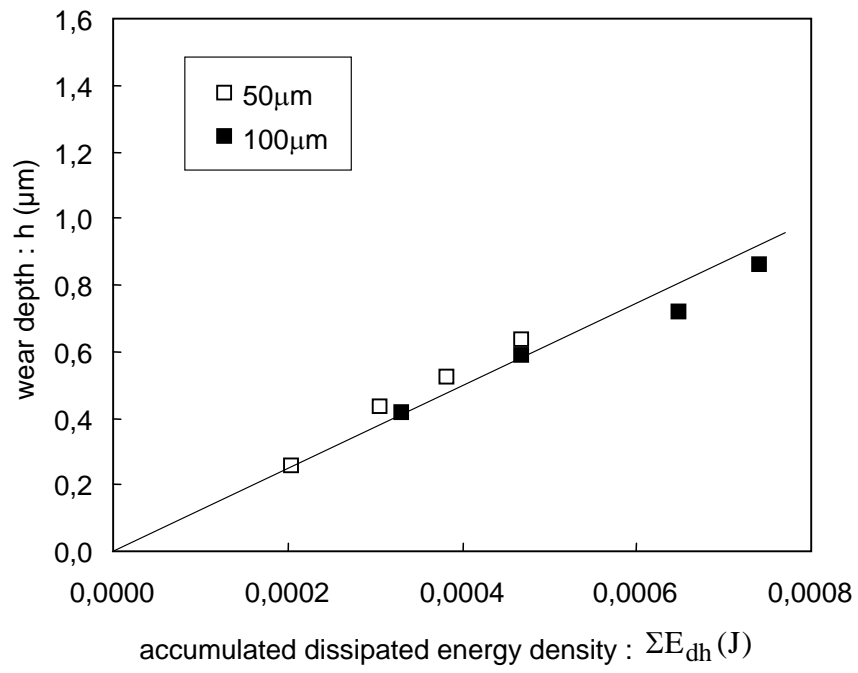


Fig. 7

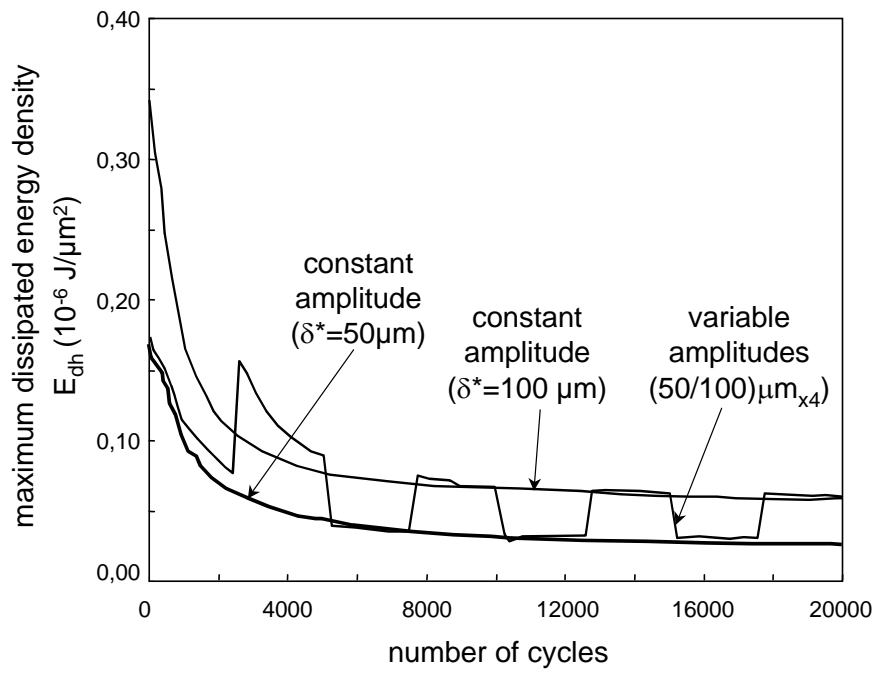


Fig. 8

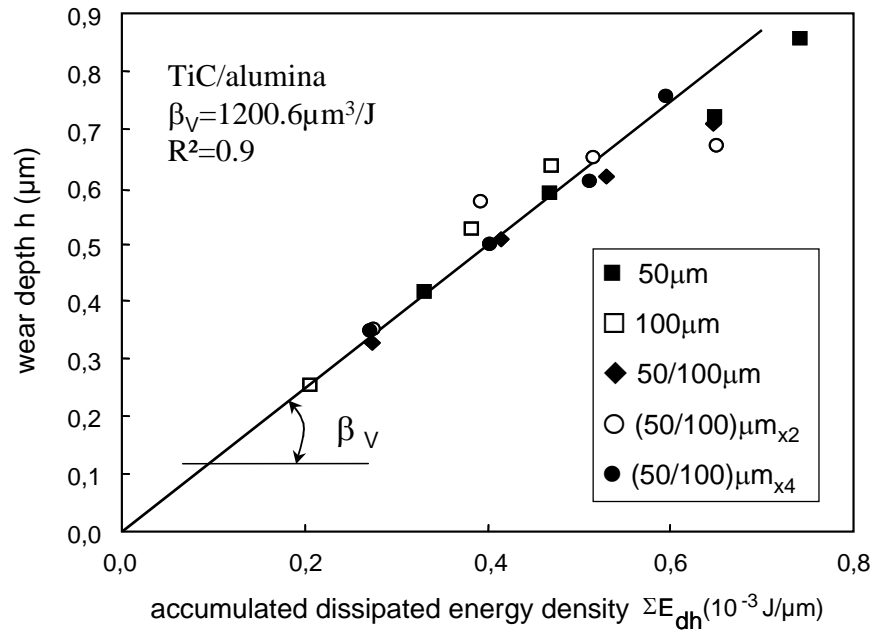


Fig. 9

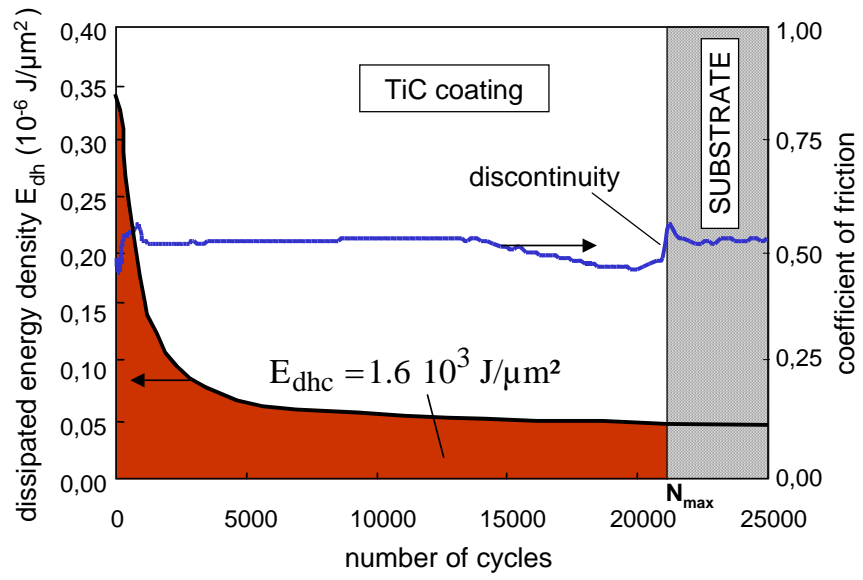


Fig. 10

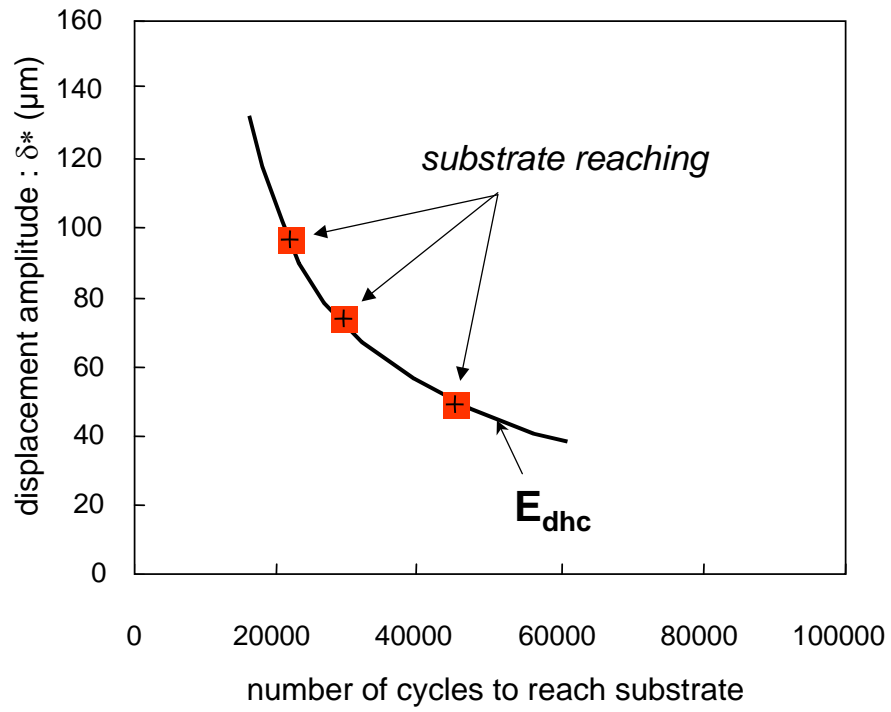


Fig. 11